The missing link in EBV immune evasion

Quinn, Laura L; Williams, Luke R; White, Claire; Forrest, Calum; Zuo, Jianmin; Rowe, Martin

DOI:
10.1128/JVI.02183-15

Document Version
Peer reviewed version

The missing link in EBV immune evasion: the BDLF3 gene induces ubiquitination and downregulation of MHC class I and MHC class II

Laura L Quinn, Luke R Williams, Claire White, Calum Forrest, Jianmin Zuo[#], Martin Rowe

Institute of Immunology & Immunotherapy (III), College of Medical & Dental Sciences, University of Birmingham, B15 2TT, UK.

Corresponding Author: email, J.Zuo@bham.ac.uk

Running Title: BDLF3, the missing link in EBV immune evasion

Abstract word count- 213

Main text word count- 5945

Abstract

The ability of Epstein-Barr virus (EBV) to spread and persist in human populations relies on a balance between host immune responses and EBV immune-evasion. $CD8^+$ cells specific for EBV late lytic cycle antigens show poor recognition of target cells compared to immediate early and early antigen-specific $CD8^+$ cells. This phenomenon is in part due to the early EBV protein, BILF1, whose immunosuppressive activity increases with lytic cycle progression. However, published data suggest the existence of a hitherto unidentified immune-evasion protein further enhancing protection against late EBV antigen-specific $CD8^+$ cells. We have now identified the late lytic gene, BDLF3, as the missing link accounting for the efficient evasion during late lytic cycle. Interestingly, BDLF3 also contributes to evasion of $CD4^+$ cell responses to EBV. We report that BDLF3 down-regulates expression of surface MHC class I and class II molecules in the absence of any effect upon other surface molecules screened, including CD54 (ICAM-1) and CD71 (Transferrin receptor). BDLF3 both enhanced internalization of surface MHC molecules and reduced the rate of their appearance at the cell surface. The reduced expression of surface MHC molecules correlated with functional protection against $CD8^+$ and $CD4^+$ T cell recognition. The molecular mechanism was identified as BDLF3-induced ubiquitination of MHC molecules and their subsequent downregulation in a proteasomal dependent manner.

Importance

Immune-evasion is a necessary feature of viruses that establish life-long persistent infections in the face of strong immune-responses. EBV is an important human pathogen whose immune evasion mechanisms are only partly understood. Of the EBV immune-evasion mechanisms identified to date, none could explain why $CD8^+$ T cell responses to late lytic cycle genes are so infrequent and, when present, recognize lytically-infected target cells so poorly relative to $CD8^+$ T cells specific for early lytic cycle antigens. The present work identifies an additional immune-evasion protein, BDLF3 that is expressed late in lytic cycle and impairs $CD8^+$ T cell recognition by targeting cell surface MHC class I molecules for ubiquitination and proteasomal dependent downregulation. Interestingly, BDLF3 also targets MHC class II molecules, to impair $CD4^+$ T cell recognition. BDLF3 is therefore a rare example of a viral gene that impairs both the class I and class II MHC antigen presenting pathways.

Introduction

Epstein-Barr virus (EBV) is a γ-herpesvirus found in more than 90% of the human population. Primary infection with EBV is usually followed by establishment of lifelong latent infection with occasional reactivation (1). The balance between host immune responses, including $CD4^+$ and $CD8^+$ T cells, and viral immune evasion of these responses is key to the spread and survival of EBV in human populations. Passive evasion through the ability to establish antigenically silent latent infections is an important characteristic of all herpesviruses, including EBV. In addition, active evasion mechanisms are an important feature of herpesviruses. As these active evasion mechanisms are predominantly observed during the lytic phase of the herpesvirus life-cycle, they are presumed to be particularly important for enabling virus spread. There have been a number of EBV encoded immune evasion genes identified that are expressed in lytic cycle and target the MHC class I or class II antigen presentation pathways (2, 3). Those genes responsible for interfering with MHC class I antigen presentation include BGLF5, BNLF2a and BILF1 which each act upon different elements of the MHC class I antigen presentation pathway (3-7). The EBV encoded proteins BGLF5, BZLF1 and gp42 have been shown to interfere with MHC class II antigen presentation (5, 8-10).

The above-mentioned MHC class I evasion genes encoded by EBV have been well studied and shown to act via different mechanisms upon different elements of the MHC class I antigen presentation pathway. Briefly, BGLF5 is a host shut off protein that has been shown to induce the degradation of MHC class I mRNA, thereby reducing cell

surface MHC class I peptide presentation (5, 11). BILF1 is known to target both cell surface MHC class I molecules and those on route to the surface for degradation thus reducing the presentation of peptides to $CD8^+$ T cells (7, 12, 13). Finally, BNLF2a inhibits the function of the transporter associated with antigen processing (TAP), which reduces the supply of peptides for loading on to MHC class I molecules, thus reducing the level of MHC class I:peptide presentation to $CD8^+$ T cells (4, 14, 15).

Our group recently investigated the relevance of BGLF5, BNLF2a and BILF1 immune evasion genes in the context of lytic virus infection (16). It was concluded that BGLF5 in fact plays a minimal role in protecting EBV infected cells against T cell recognition, and that BNLF2a plays an important role of protecting cells during the immediate early and early stages of lytic cycle, contributing little protection at late stage lytic cycle (IE>E>>L) (14, 16). BILF1 was shown to contribute minimal protection during immediate early stage lytic cycle, a reasonable level of protection during early stage lytic cycle and a more dramatic level of protection was observed during late stage lytic cycle (IE<E<<L) (16). This investigation revealed a level of co-operation between EBV encoded MHC class I immune evasion genes in order to protect cells from $CD8^+$ T cell recognition. However, $CD8^+$ T cell responses to late lytic cycle antigens still recognize lytically-infected target cells relatively poorly, even in the absence of BILF1 expression. (16, 17). This implies that another as yet unidentified immune evasion gene or genes may be functioning late in lytic cycle.

In comparison to what is known about the immune evasion of MHC class I antigen presentation, the evasion of MHC class II antigen presentation by EBV is less well

understood. Over-expression of the host shut off protein, BGLF5 has been shown to result in a reduced level of surface MHC class II (5). In addition, the immediate early protein BZLF1 has been shown to interfere with MHC class II antigen presentation by modulating the expression of cell surface invariant chains (8). A third EBV encoded gene, BZLF2 (gp42), has been shown to interfere with MHC class II antigen presentation to $CD4^+$ T cells by sterically hindering MHC class II interaction with the T cell receptor, thus blocking $CD4^+$ T cell recognition (9, 10). To date, no other EBV proteins have been identified as potential $CD4^+$ T cell immune evasion proteins.

The present study sought to identify novel candidate EBV genes responsible for interfering with MHC class I antigen presentation during late phase lytic cycle, and thus providing an explanation for the pronounced immune evasion observed at that stage in the lytic cycle. Screening experiments revealed that the late lytic protein, BDLF3, whose functions are unknown (18-20), was able to impair MHC class I antigen presentation. Unexpectedly, BDLF3 also impaired $CD4^+$ T cell recognition of MHC class II presented peptides. The molecular mechanism for the effect of BDLF3 on antigen presentation involved ubiquitination and proteasomal dependent downregulation of surface MHC class I and class II molecules.

Materials and methods

Plasmids

The previously described (7) expression plasmid pCDNA3-IRES-GFP, a kind gift from Professor Emmanuel Wiertz (Utrecht Medical Center, Netherlands), was used to subclone and express a selection of EBV genes. The p509 expression plasmid for BZLF1, a kind gift from Professor Paul Farrell (Imperial College London, UK), has also been described (11) as has the cytoplasmic EBNA1 expression vector (21). The retroviral plasmid PLZRS-NGFR, also a kind gift from Professor Emmanuel Wiertz, was used to subclone PLZRS-BDLF3-NGFR and both were used in transient transfections to allow for in house sorting of transfected cells, on the expression of surface truncated nerve growth factor receptor (NGFR).

Cells, transfections and electroporations

The MJS (Mel JuSol) melanoma-derived cell line (22), and the EBV negative Burkitt lymphoma cell line DG75 (23) were maintained in RPMI 1640 supplemented with 10% fetal calf serum (FCS). CIITA-293 cells are HEK-293 cells stably expressing CIITA (24) and were a kind gift from Dr Andrew Hislop, University of Birmingham. These were maintained in Dulbecco's modified Eagle's medium (DMEM) supplemented with 10% FCS. The myelogenous leukemia cell line K562, transduced to express either HLA-A2, -B35, -Cw1, -DR or –DQ (a kind gift from Professor Emmanuel Wiertz, Utrecht) were maintained in RPMI 1640 supplemented with 10% FCS plus 400μg/ml of geneticin (Invitrogen). EBV specific $CD4^+$ and $CD8^+$ T cell clones were grown in RPMI 1640

supplemented with 10% FCS, 5% human serum, 30% supernatant from the interleukin-2 producing MLA 144 cell line (25) and 50 U/ml recombinant interleukin-2, as described previously (17).

Transient transfection of MJS and 293-CIITA cells with plasmid DNA was performed using lipofectamine 2000 (Invitrogen) according to the manufacturer's instructions.

Transient expression of plasmid DNA using DG75 cells and K562 cells was performed by electroporating cells at 290V and 950μF in 4mm gap cuvettes. In some experiments, cells transiently transfected with NGFR expressing plasmids were positively selected for the surface expression of NGFR using MACSelect NGFR-Transfected Cell Selection kits, as per manufacturer's protocol (Miltenyi Biotec).

Antibodies

For immunoprecipitation experiments and for internalization/appearance assays, unconjugated W6/32 and L243 murine monoclonal antibodies (MAbs) to human MHC molecules were obtained from Biolegend: W6/32 (26) recognizes native β_2 microglobulin-associated MHC class I complexes (HLA-A, -B and –C alleles); and L243 for HLA-DR. For flow cytometry experiments, APC- and PE- conjugated antibodies to HLA class I (W6/32), HLA-DR (L243), ICAM1/CD54 (HCD54) and transferrin receptor/CD71 (TfR, CY1G4) were purchased from Biolegend. For western blotting, mouse anti-ubiquitin antibody (P4D1) MAb was purchased from Biolegend. Goat antibodies to calregulin were purchased from Santa Cruz Biotechnology. The BZ.1 murine MAb specific for the EBV BZLF1-encoded protein was generated by our

laboratory (27). The rabbit anti-BDLF3 (V8) serum was a kind gift from Dr. L.Hutt-Fletcher (19).

Flow cytometry analysis of cell surface MHC class I and class II molecules

Cell surface expression of MHC class I and class II was determined by staining cells with APC- or PE- conjugated anti-HLA class I or class II antibodies and detected on BDbiosciences Accuri C6 Flow Cytometer. Data were analyzed using FlowJo software (TreeStar).

The kinetics of internalization and appearance of cell surface MHC molecules were determined essentially as described previously (12).To assay the kinetics of surface MHC class I and class II internalization, MJS cells were incubated on ice with saturating amounts of anti-MHC class I (W6/32) or anti-MHC class II (L243) MAbs. Cells were then washed three times in phosphate-buffered normal saline (PBS) and placed in culture medium at 37ºC for 60 mins. Aliquots of cells were taken at those times shown in results, and were rapidly cooled to 0ºC to inhibit further membrane trafficking. The level of W6/32 or L243 MAb remaining at the cell surface was then analyzed by staining cells with APC-conjugated goat anti-mouse IgG2a antibody (Biolegend). Cells were analyzed using flow cytometry.

To assay the kinetics of MHC class I and II appearance, MJS cells were again incubated with saturating amounts of W6/32 or L243 for 60 mins on ice. Cells were washed three times in PBS and then placed in warm culture medium at 37ºC for 60min, cells were analyzed at times indicated in results. After cooling to 0ºC, to prevent further appearance of molecules at the surface through membrane trafficking, cells were

stained with APC-conjugated W6/32 or APC-conjugated L243 and analyzed using flow cytometry. These directly conjugated anti-MHC detection antibodies will only bind to MHC molecules that have appeared since the excess unconjugated blocking antibody was washed away immediately prior to beginning the incubations in warmed medium. Note that the MHC molecules newly-arrived at the cell surface are likely to be a mixture of de-novo synthesized molecules arriving at the surface for the first time, and recycled molecules that had previously been endocytosed.

Flow cytometric analysis of whole cell (intracellular) proteins

Intracellular staining for HLA class I and class II was performed to quantify the total cellular levels of these proteins. Washed pellets of $0.5x10^6$ cells were first fixed using 100µl Ebiosciences intracellular (IC) fixative for 1h on ice, followed by permeabilization using 100µl (0.2%) Triton X-100 and further 30 min incubation on ice. After washing in PBS, cells were incubated with appropriate conjugated antibody for 1h at 37ºC. Cells were then washed in PBS and analyzed using flow cytometry.

T cell function assays

'RAK' $CD8^+$ T cell clones specific for the **RAK**FKQLL peptide originating from BZLF1 protein, and 'SNP' $CD4^+$ clones specific for the **SNP**KFENIAEGLRVLLARSH epitope from ENBA1 protein, were generated as previously described (16). Targets for RAK-specific $CD8^+$ T cells were generated by co-transfection of MJS cells with BZLF1 and control-GFP or BDLF3-GFP expression plasmids. At 24h post transfection, cells were used as targets for RAK specific $CD8^+$ T cell clones. T cell recognition was determined

by interferon gamma (IFN-γ) enzyme-linked immunosorbant assay (ELISA) using a previously described protocol (16). Targets for SNP-specific $CD4^+$ T cell clones were generated by transfection of MJS cells with the cytoplasmic EBNA1 expression plasmid, EBNA1ΔNLS, which generates a target protein that is efficiently processed via the MHC antigen presentation pathway (21). At 24h post-transfection cells were re-seeded and 24h later these cells were transfected with control-NGFR or BDLF3-NGFR expression plasmids. After a further 24h, cells were harvested and sorted as described above and the recognition of these target cells by SNP-specific $CD4^+$ T cell clones was determined by IFN-γ ELISA.

Immunoprecipitation

Positively selected control-NGFR and BDLF3-NGFR expressing MJS cells ($2x10^6$) were used for surface MHC class I and class II immunoprecipitation. Cells were incubated for two hours on ice with anti-HLA class I Mab (W6/32) or anti-HLA class II Mab (L243), then washed and lysed using 400µl of NP-40 buffer (0.5% Nonidet P-40, 5mM $MgCl_2$ and 50mM Tris-HCl, pH7.5) with protease inhibitor cocktail (Sigma P8340) at 4ºC for 45 min. Nuclei and insoluble debris were removed by centrifugation, and the supernatants were incubated with 20µl Dynabeads Protein A and 20µl Dynabeads Protein G (Invitrogen) at 4ºC overnight. Beads were then washed four times with NET buffer (0.5% NP-40, 150mM $NaCl_2$, 5mM EDTA and 50mM Tris-HCl, pH 7.5) and the precipitated proteins were eluted by boiling in reducing sample buffer for 5 min. Finally, samples were separated by SDS-PAGE on 4-12 % Bis-Tris NuPage mini-gels with morpholinepropanesulfonic acid (MOPS) electrolysis buffer (Invitrogen).

Western blotting

Total cell lysates were denatured in reducing sample buffer and then sonicated and heated to 100ºC for 5 min. Solubilized proteins equivalent to $2x10^5$ cells/20µl sample were separated by SDS-polyacrylamide gel electrophoresis (SDS-PAGE) on to 4-12% acrylamide gradient bis-Tris NuPage minigels with MOPS running buffer (Invitrogen).

Results

The late lytic gene BDLF3 is identified as an immune evasion protein

As previously demonstrated, EBV encodes a number of immune evasion genes that co-operate to afford the protection of EBV infected cells against recognition by $CD8^+$ T cells during lytic cycle. However, it has been hypothesized that an as yet unidentified EBV lytic gene may be responsible for the ultimate protection of EBV infected cells during late lytic cycle (16). In order to identify other potential EBV immune evasion proteins involved in protecting infected cells against $CD8^+$ T cell recognition, more than 25 EBV genes expressed during lytic cycle were transiently expressed in MJS cells using bicistronic plasmid vectors that co-expressed GFP with the test gene (Supplementary Fig. 1A). The expression of GFP protein allowed for the identification of transfected cells using flow cytometry. At 24h post-transfection, flow cytometric analysis was used to analyse surface expression levels of MHC class I on GFP positive cells. Of all EBV lytic genes included in this screen the only protein that reproducibly affected surface levels of MHC class I was BDLF3 (Fig. 1A). Fig. 1A shows a representative selection of these screens. As a control, the level of surface MHC class II was also analyzed in this screen (Supplementary Fig. 1B). Interestingly, BDLF3 also affected the surface expression of MHC class II (Fig. 1B).

BDLF3 has previously been classified as a late expressed lytic protein (19). We confirmed the late expression kinetics using the EBV positive cell line, AKBM (9) that can be induced in to lytic cycle by cross linking of the B cell receptor. Following induction, aliquots of induced AKBM cells were taken at 0h, 1h, 6h, 12h, 24h, and 48h

time points and immunoblotting was performed in order to detect the expression of BDLF3 and the immediate early protein BZLF1. As shown in Fig. 1C, BDLF3 protein expression is detected weakly at 12hr post induction but with stronger expression seen at 24hr. These expression kinetics are consistent with previous findings (19) and suggests that BDLF3 could potentially be the 'missing link' immune evasion protein responsible for interfering with MHC class I antigen presentation during late stage lytic cycle to protect these cells against $CD8^+$ T cell recognition. In addition, the effect on expression of MHC class II molecules raised the possibility that BDLF3 also plays a role in $CD4^+$ T cell immune evasion. To confirm that the levels of BDLF3 protein expression in our transfected cells were physiologically relevant, BDLF3 protein expression levels in the transfected MJS cells was compared with BDLF3 expression level in induced AKBM cells after adjusting for the percentage of GFP^+ cells in MJS cells and percentage of VCA^+ cells in induced AKBM cells. Quantification of western blots (Supplementary Fig. 2) showed that the expression of BDLF3 in MJS was around 70% of that expressed in induced AKBM cells.

In order to confirm that BDLF3 acts specifically on MHC class I and MHC class II, MJS cells transiently expressing BDLF3 were harvested at 24hr post-transfection and were analyzed in more detail using flow cytometry to detect surface levels of MHC class I, MHC class II, and other cell surface proteins. The results in Fig. 2A indicated that BDLF3 expressing cells (dashed line) exhibit a 60% decrease in surface MHC class I mean fluorescence intensity (MFI) compared to control cells (solid black line). A similar result was observed for surface levels of MHC class II on BDLF3 positive cells (Fig. 2B), where there was a reduction of 50% in MHC class II MFI. Importantly, the levels two

other surface proteins tested, Transferrin receptor (TfR; Fig. 2C) and ICAM1, (Fig. 2D) were not affected by the expression of BDLF3.

Since B cells are the natural reservoir for EBV, we next investigated the phenotype of BDLF3 in B cells. To this end, the effect of transient BDLF3 expression on surface MHC molecules on the EBV negative B cell line, DG75 was investigated using flow cytometry. In this instance, the control of ICAM1 could not be included as its expression on DG75 cells is negligible; therefore the effect of BDLF3 on expression of CD19 was analyzed along with TfR expression. As shown in Fig. 2E-H, results similar to those seen in MJS cells were obtained. BDLF3 expressing DG75 cells showed a 43% reduction in the MFI of MHC class I (Fig. 2E) and a 30% reduction in MHC class II (Fig. 2F) compared to control cells not expressing BDLF3. There was no observed effect of BDLF3 on the expression of surface TfR (Fig. 2G) or CD19 (Fig. 2H).

BDLF3 induces downregulation of all screened MHC class I and MHC class II alleles

Since some viral immune evasion genes, including BILF1, have been shown to preferentially target specific HLA class I alleles (13), we next sought to investigate the HLA-specificity of BDLF3. To do so, MHC class I negative K562 cells engineered to stably express HLA-A2, -B35 or –Cw1 were transiently transfected to express either BDLF3 or a control vector. At 24h post-transfection the surface level HLA-A2, -B35 and –Cw1 on positively transfected cells was detected using flow cytometry. As shown in Fig. 3A, cells expressing BDLF3 showed a decrease in the cell surface level of HLA-A2

(upper histograms) (27% reduction in MFI), HLA-B35 (middle histograms) (34% reduction in MFI) and HLA-Cw1 (lower histograms) (26% reduction in MFI) compared to control cells. A similar approach was then used to test the specificity of BDLF3 for HLA class II alleles. Here, HLA class II negative HEK-293 cells engineered to stably expressing CIITA, thus driving the surface expression of HLA-DR and -DQ, were transiently transfected to express BDLF3 or control vector. Similar to that seen for HLA class I alleles, BDLF3 induced a reduction in both HLA-DR (47% reduction in MFI) (Fig. 3B, upper histograms) and HLA DQ (32% reduction in MFI) (Fig. 3B, lower histograms) compared to control transfected cells. In all examples the level of surface TfR remained similar between BDLF3 and control transfected cells (data not shown). These results indicate that BDLF3 is not selective in down-regulating HLA molecules but instead acts more broadly to down regulate all HLA class I and HLA class II molecules.

BDLF3 mediated reductions in surface MHC class I and class II confers protection against both $CD8^+$ and $CD4^+$ T cell recognition

Since BDLF3 induces a reduction in the level of surface MHC class I and class II molecules, we next investigated whether BDLF3 expression provided protection against recognition by EBV-specific $CD8^+$ and $CD4^+$ T cells. In order to address this, the HLA-B8 positive cell line MJS cells, were co-transfected with BZLF1 and either BDLF3-GFP or control-GFP vector plasmids (Fig. 4A). At 24h post-transfection these cells were used as targets in a T cell assay with $CD8^+$ T cell clones restricted through HLA-B8 and specific for the peptide RAKFKQLL, contained within the BZLF1 antigen. T cell

316 recognition was measured as IFN-γ release using IFN-γ ELISA. As shown in one
317 representative experiment (n=3) in Fig. 4A, the expression of BDLF3 resulted in a
318 significant decrease in IFN-γ release by RAK-specific T cell clones, from ~1100pg/ml to
319 ~500pg/ml. The BDLF3-mediated reduction in BZLF1-specific $CD8^+$ T cell recognition
320 was not due to any change in the expression of BZLF1 target protein expression (Fig.
321 4B).

322 In order to investigate the ability of BDLF3 to protect cells against recognition by $CD4^+$ T
323 cells, a similar method was employed. Here, MJS cells stably expressing the HLA class
324 II allele DR51 were transfected to express cytoplasmic EBNA1 for 48h and either
325 BDLF3-NGFR or control-NGFR vector for a further 24hr (Fig. 4C). Cells were then
326 sorted on expression of NGFR and subsequently used as targets for a $CD4^+$ T cell
327 clones specific for the HLA-DR51 restricted epitope SNPKFENIAEGLRVLLARSH,
328 contained within EBNA1. As shown in Fig. 4C, the expression of BDLF3 resulted in a
329 decrease in T cell recognition (IFN-γ release) by SNP-specific $CD4^+$ T cell clones from
330 ~1300pg/ml to ~900pg/ml, compared to control cells. The BDLF3-mediated reduction in
331 EBNA1-specific $CD4^+$ T cell recognition was not due to any change in the expression of
332 EBNA1 target protein expression (Fig. 4D). Thus, in a similar pattern to those results
333 seen for BDLF3 protection against $CD8^+$ T cell recognition, BDLF3 induced reduction in
334 surface MHC class II molecules also correlated with protection against $CD4^+$ T cell
335 recognition.

These data show that BDLF3 induced reduction in cell surface MHC class I and class II is functional in protecting BDLF3 expressing cells against recognition by both $CD8^+$ and $CD4^+$ T cells.

BDLF3 downregulates surface MHC molecules more dramatically than total MHC molecules

To explore the mechanism of MHC class I and class II downregulation by BDLF3, we first asked whether the total cellular pool of MHC molecules was affected, or whether surface MHC molecules were selectively targeted. To this end, flow cytometry of intracellular staining of fixed and permeabilized cells was used to detect the level of whole cell MHC molecules compared to surface MHC molecules detected on impermeable viable cells. As expected, surface level MFI of MHC class I and class II were both reduced by approximately 50% on cells expressing BDLF3 compared to control cells (Fig. 5A, left-hand column). This difference was found to be significant (Fig. 5B, white bars). Interestingly, there was only a slight decrease of 10% in the MFI of whole cell MHC class I and MHC class II compared to control cells (Fig. 5A, right column) and this small reduction was not statistically significant when the results from three independent experiments were pooled and analyzed (Fig. 5B, grey bars). To confirm these findings by an independent method, control GFP expressing MJS and BDLF3-GFP expressing MJS cells were purified using Mo-flow cell sorter and the expression of total MHC-I and MHC-II was examined by western-blot. The result showed no significant difference (supplementary Fig.3), confirming the result from

intracellular flow cytometry data. Importantly, BDLF3 had no effect on surface or whole cell levels of ICAM1 expression (Figs. 5A and 5B, bottom panel).

These data show that BDLF3 affects the levels of surface MHC molecules more dramatically than it affects whole cell MHC molecules, suggesting that BDLF3 exerts its function predominantly on surface MHC class I and II rather than the intracellular fraction of these molecules.

BDLF3 induces rapid internalization and delayed appearance of MHC molecules

Since BDLF3 predominantly targets surface MHC molecules, we next examined whether it targets those MHC molecules already at the cell surface or those trafficking to the cell surface. We therefore compared the kinetics of MHC class I and class II internalization and appearance at the cell surface of BDLF3 expressing cells using flow cytometry. Representative examples are shown of MHC class I (Fig. 6A, upper) and class II (Fig. 6A, lower) internalization assays, where the percentage of MHC class I and class II remaining on the surface of BDLF3 expressing and control cells was measured over 60 minutes. Cells expressing BDLF3 showed lower levels of surface MHC remaining at the cell surface at each time point indicated, such that by 60min there were respectively 20% and 13% less surface MHC class I and MHC class II on BDLF3 expressing cells compared to control cells. These data indicate that BDLF3 induces a more rapid rate of both MHC class I and MHC class II internalization.

When a similar assay was used to measure the rate of MHC class I and class II surface appearance, BDLF3 expressing cells conversely showed a decreased rate of both MHC class I and class II surface appearance at each time point compared to control cells (Fig. 6B). By 60 min, the appearance of MHC class I and class II on BDLF3 expressing cells at time point 60min was reduced by 50% and 47% respectively in comparison to control cells. This BDLF3-mediated reduction in the rate of appearance of MHC at the surface (Fig. 6B) was noticeably greater than the accelerated rate of endocytosis (Fig.6A).

It should be noted that in all experiments rate of TfR internalization or appearance remained similar between control and BDLF3 expressing cells (data not shown). These data indicate that BDLF3 is able to both enhance endocytosis of MHC molecules at the cell surface and interfere with the trafficking of intracellular MHC molecules to the cell surface.

BDLF3 downregulation of surface MHC molecules involves ubiquitination and the proteasomal pathway

We next sought to identify the mechanism by which BDLF3 is able to enhance internalization and delay the appearance of surface MHC class I and MHC class II molecules. Our initial experiments were designed to identify which pathway BDLF3 might utilize in order to reduce the expression of surface MHC molecules. To this end, we incubated BDLF3 expressing cells with proteasomal and lysosomal inhibitors. In the absence of drug treatment, cells expressing BDLF3 showed lower levels of surface

MHC class I and II expression compared to control cells (Fig. 7A) as expected. However, when incubated with the proteasomal inhibitor, MG132, BDLF3 expressing cells showed no such reduction in surface MHC class I and MHC class II levels compared to control cells (Fig. 7B). Part abrogation of BDLF3 phenotype by MG132 was observed after 4hr treatment, but the effect of MG132 treatment was maximal after 16h (Supplementary Fig. 4). Similar results were seen when cells were treated with a second proteasomal inhibitor, bortezomib (Supplementary Fig. 5), whereas treatment with a lysosomal inhibitor, bafilomycin (Supplementary Fig. 6), did not prevent BDLF3 induced downregulation of surface MHC molecules. These data indicate that BDLF3 induced downregulation of surface MHC molecules is dependent upon the proteasomal pathway.

As BDLF3 downregulates surface MHC molecules through increased internalization and delayed appearance (Fig. 6), we next examined what effect proteasomal inhibition might have on the kinetics of MHC class I and class II internalization and appearance at the cell surface of BDLF3 expressing cells. The results showed that MG132 completely abrogated the effect of BDLF3 on both the rate of internalization (Fig 7C) and the rate of appearance (Fig.7D), demonstrating an essential role of the proteasome in BDLF3 induced MHC molecule downregulation.

Given the essential role that the proteasome plays in BDLF3 induced reduction of surface MHC molecules, and that ubiquitination is an important component of the proteasomal pathway, we next assessed whether BDLF3 induces ubiquitination of

surface MHC molecules. To this end, MJS cells were transfected with various expression vectors including BDLF3, control vector and ubiquitin (Fig. 7E, F). These cells were then incubated with or without the proteasomal inhibitor, MG132. At 24h post-transfection, surface MHC class I or MHC class II molecules were immunoprecipitated from BDLF3 expressing or control cells and resulting immunoblots were probed with ubiquitin-specific antibodies. As shown in Fig. 7, poly-ubiquitinated high molecular weight bands appeared in immunoblots for immunoprecipitated MHC class I (Fig. 7E) and MHC class II (Fig. 7F) in BDLF3 expressing cells treated with MG132. These ubiquitin-reactive bands were less pronounced both in control cells treated with MG132 and in BDLF3-expressing cells not treated with MG132.

Discussion

This study reveals the identity and mechanism of novel immune evasion gene, BDLF3, which induces downregulation of not only cell surface MHC class I but also MHC class II, to the extent that antigen recognition by both $CD8^+$ and $CD4^+$ virus-specific T cells is functionally impaired. The BDLF3 protein was first identified a number of years ago as the glycoprotein gp150, which is located at the cell membrane and in the virion, is not essential for EBV replication, and hitherto had no known function (18-20). Our study now allows a function to be assigned to the BDLF3 protein.

The identification of BDLF3 as an immune evasion protein has an important impact on our knowledge of the T cell response to lytic EBV antigens and the protection of EBV infected cells from recognition by these T cells. EBV lytic cycle involves the synchronous expression of more than 60 viral proteins, many of which elicit strong $CD4^+$ and $CD8^+$ T cell responses, but various immune-evasion mechanisms enable EBV to persist as a lifelong infection. For $CD8^+$ T cell responses to lytic cycle antigens, there is a pattern of immunodominance that correlates with the efficiency of antigen presentation during lytic cycle. An earlier study by our group revealed that the known immune evasion genes, BGLF5, BNLF2a and BILF1 act in co-operation to afford protection to EBV infected cells against lytic specific CD8 T^+ cell recognition. However, the ultimate protection that is seen in late phase lytic cycle could not be fully explained by the action of these known evasion genes (16). The identification of BDLF3, which is expressed during late stage lytic cycle, as a potent inhibitor of the MHC class I antigen presentation pathway makes it a prime candidate for the ‘missing link’ immune evasion

453 protein responsible for protecting EBV infected cells from $CD8^+$ T cell responses during
454 late stage lytic cycle.

455 Another important feature of BDLF3 is its ability to induce MHC class II downregulation
456 and evade $CD4^+$ T cell recognition. Evidence is accumulating in the literature showing
457 that viruses target multiple points on the MHC class II antigen presentation pathway,
458 including: suppression of CIITA (28, 29), diversion or degradation of DR molecules
459 during membrane transport (30) and direct targeting of the CD74 (invariant chain)
460 chaperone of DR (8). Two viral genes expressed during EBV lytic cycle have been
461 reported to manipulate MHC class II antigen presentation pathway. BZLF1 induces a
462 marked downregulation of surface CD74 to impair antigen presentation and $CD4^+$ T cell
463 recognition (8), and Gp42 sterically inhibits interactions between TCR on the $CD4^+$ T
464 cell with MHC-II peptide complexes (10). The identification of BDLF3 as a novel MHC
465 class II evasion gene from EBV indicates that, similarly to interference with MHC class I
466 antigen presentation, interference with MHC class II antigen presentation very likely
467 involves the cooperative action of multiple evasion genes.

468 The fact that BDLF3 is an EBV late lytic cycle protein, suggests that it would help to
469 provide enhanced protection of the virus-producing cells prior to release of mature
470 virions. In addition, as BDLF3 can be detected in the EBV virion (31), this raises the
471 possibility that BDLF3 can act immediately after new infections of B cells to modulate
472 recognition by existing EBV specific $CD4^+$ T cells. Considering the important role of
473 MHC class II molecules and gp42 in EBV infection, and also the observation that
474 BDLF3 knock-out EBV virus particles can infect epithelial cells better than B cells (18),

we can propose a potential role of BDLF3 in the EBV infection. BDLF3 expression results in decreased MHC class II expression at the surface of lytically replicating cells, reducing the amount of MHC class II available to bind gp42. We would therefore predict that BDLF3 knockout virions may contain less envelope gp42 than wild type EBV, with a consequent enhanced ability to infect epithelial cells.

Our data indicate that the mechanism of BDLF3 interference with the appearance of MHC molecules at, and internalization from, the cell surface, involves ubiquitination of MHC molecules and proteasome-dependent pathways. The targeting of MHC molecules for ubiquitination has been described for other viral immune evasion proteins, but the mechanism of action of BDLF3 is clearly distinct. An example is the K3 and K5 proteins encoded by Kaposi's sarcoma-associated herpesvirus (KSHV), which function as two membrane-bound E3 ubiquitin ligases and have been shown to facilitate the rapid endocytosis and subsequent degradation of MHC class I by inducing ubiquitination (32-37). Unlike K3 and K5, there is no evidence to show that BDLF3 itself is an E3 ubiquitin ligase, therefore it is very likely that BDLF3 functions via a different mechanism. Indeed in terms of the MHC class I downregulation, BDLF3 can affect all MHC class I alleles we studied, whereas K5 affects HLA-A and –B but has a weak effect on HLA-C, while K3 downregulates all HLA class I alleles (33). More importantly, KSHV K3 and K5 can downregulate a range of other surface proteins including B7-2, CD54 (ICAM-1), CD1d, CD31 (PECAM-1), IFN-γR1, MICA/B, BST-2, ALCAM, Syntaxin-4 (38-42). In contrast we found that BDLF3 targets MHC-I and MHC-II, but not CD54 (Fig. 2) or MICA/B (data not shown). Another distinguishing feature of BDLF3 is that whilst the surface levels of MHC class I and class II were reduced by around 50%, there

was a minimal decrease of whole cell MHC class I and MHC class II (Fig. 5A, and Supplementary Fig. 3). That BDLF3 can induce a 50% reduction in surface MHC molecules against a reduction of less than 10% of the whole cell MHC molecules reflects the fact that there is relatively large reservoir of MHC class I and MHC class II inside the cells. Therefore, the 10% reduction in whole cell MHC class I and II could represent the complete degradation of the 50% of MHC class I and II that is lost from the surface in the presence of BDLF3.

Whilst BDLF3 does not function as ubiquitin E3 ligase, it does nevertheless downregulate surface MHC class I and MHC class II through inducing ubiquitination. How might this be? One possible explanation is that it may recruit other cellular E3 ubiquitin ligase proteins such as members of the membrane-associated RING-CH (MARCH) proteins, the cellular orthologues of K3 and K5. These proteins have been implicated in the regulation of cell surface molecules including MHC class I, MHC class II, ICAM and transferrin receptor (36, 43-46). Indeed, the overexpression of MARCH-IV and MARCH-IX proteins induces ubiquitination and rapid internalization of MHC class I (43). Numerous MARCH proteins have been identified that target MHC class I or MHC class II although, at the time of writing, no single known MARCH protein induces the ubiquitination of both MHC class I and class II without affecting other surface markers that are left unaffected by BDLF3 (47). Our preliminary experiments have not been able to demonstrate co-immunepreciptation of MHC molecules with BDLF3 (data not shown). Thus BDLF3 may recruit an as of yet unidentified MARCH family protein or perhaps several of these proteins. If so, then the specificity of BDLF3 would be due to the target

molecules of these recruited proteins. Future work will be aimed at resolving these possibilities.

Considering the data that we have obtained for BDLF3, and the features that distinguish the effects of BDLF3 from previously characterized immune evasion proteins, we postulate that its mechanism of action is broadly as follows. As BDLF3 reduces the rate of appearance of MHC molecules at the cell surface to a greater extent than it increases the rate of endocytosis (Fig.6) we suppose that the reduced rate of appearance must be due at least in part to an effect on de novo synthesized MHC molecules trafficking to the surface. Therefore, BDLF3 targets for ubiquitination both de novo synthesized and recycling endocytosed MHC molecules. These ubiquitinated MHC molecules are directed for proteasomal degradation or, in the presence of proteasomal inhibitors, accumulate at the cell surface. The finer details of the biochemical mechanisms, and the identity of the ubiquitin ligases involved, remain to be resolved.

The acquisition of immune evasion proteins has played a critical role in the evolution of viruses. It is interesting to note that an EBV homolog, the marmoset lymphocryptovirus (maLCV), which naturally infects new world nonhuman primates, lacks BDLF3. This may be relevant to the fact that serological studies reveal maLCV infection in marmosets to be much less ubiquitous than EBV in humans (48, 49). It might therefore be speculated that the acquisition of BDLF3 immune evasion functions is a later evolutionary event that contributes to the success of EBV in successfully colonizing the vast majority of the human population.

Reference

1. **Rickinson AB, E. Kieff.** 2007. Epstein-Barr Virus. In D. M. Knipe and P. M. Howley (ed.), Fields Virology **2. Lippincott Williams & Wilkins, Philadelphia, PA:**2655-2700. .
2. **Ressing ME, Horst D, Griffin BD, Tellam J, Zuo J, Khanna R, Rowe M, Wiertz EJ.** 2008. Epstein-Barr virus evasion of CD8(+) and CD4(+) T cell immunity via concerted actions of multiple gene products. Semin Cancer Biol **18:**397-408.
3. **Rowe M, Zuo J.** 2010. Immune responses to Epstein-Barr virus: molecular interactions in the virus evasion of CD8+ T cell immunity. Microbes Infect **12:**173-181.
4. **Hislop AD, Ressing ME, van Leeuwen D, Pudney VA, Horst D, Koppers-Lalic D, Croft NP, Neefjes JJ, Rickinson AB, Wiertz EJ.** 2007. A CD8+ T cell immune evasion protein specific to Epstein-Barr virus and its close relatives in Old World primates. J Exp Med **204:**1863-1873.
5. **Rowe M, Glaunsinger B, van Leeuwen D, Zuo J, Sweetman D, Ganem D, Middeldorp J, Wiertz EJ, Ressing ME.** 2007. Host shutoff during productive Epstein-Barr virus infection is mediated by BGLF5 and may contribute to immune evasion. Proc Natl Acad Sci U S A **104:**3366-3371.
6. **Zeidler R, Eissner G, Meissner P, Uebel S, Tampe R, Lazis S, Hammerschmidt W.** 1997. Downregulation of TAP1 in B lymphocytes by cellular and Epstein-Barr virus-encoded interleukin-10. Blood **90:**2390-2397.
7. **Zuo J, Currin A, Griffin BD, Shannon-Lowe C, Thomas WA, Ressing ME, Wiertz EJ, Rowe M.** 2009. The Epstein-Barr virus G-protein-coupled receptor contributes to immune evasion by targeting MHC class I molecules for degradation. PLoS Pathog **5:**2.
8. **Zuo J, Thomas WA, Haigh TA, Fitzsimmons L, Long HM, Hislop AD, Taylor GS, Rowe M.** 2011. Epstein-Barr virus evades CD4+ T cell responses in lytic cycle through BZLF1-mediated downregulation of CD74 and the cooperation of vBcl-2. PLoS Pathog **7:**22.
9. **Ressing ME, van Leeuwen D, Verreck FA, Keating S, Gomez R, Franken KL, Ottenhoff TH, Spriggs M, Schumacher TN, Hutt-Fletcher LM, Rowe M, Wiertz EJ.** 2005. Epstein-Barr virus gp42 is posttranslationally modified to produce soluble gp42 that mediates HLA class II immune evasion. J Virol **79:**841-852.
10. **Ressing ME, van Leeuwen D, Verreck FA, Gomez R, Heemskerk B, Toebes M, Mullen MM, Jardetzky TS, Longnecker R, Schilham MW, Ottenhoff TH, Neefjes J, Schumacher TN, Hutt-Fletcher LM, Wiertz EJ.** 2003. Interference with T cell receptor-HLA-DR interactions by Epstein-Barr virus gp42 results in reduced T helper cell recognition. Proc Natl Acad Sci U S A **100:**11583-11588.
11. **Zuo J, Thomas W, van Leeuwen D, Middeldorp JM, Wiertz EJ, Ressing ME, Rowe M.** 2008. The DNase of gammaherpesviruses impairs recognition by virus-specific CD8+ T cells through an additional host shutoff function. J Virol **82:**2385-2393.
12. **Zuo J, Quinn LL, Tamblyn J, Thomas WA, Feederle R, Delecluse HJ, Hislop AD, Rowe M.** 2011. The Epstein-Barr virus-encoded BILF1 protein modulates immune recognition of endogenously processed antigen by targeting major histocompatibility complex class I molecules trafficking on both the exocytic and endocytic pathways. J Virol **85:**1604-1614.
13. **Griffin BD, Gram AM, Mulder A, Van Leeuwen D, Claas FH, Wang F, Ressing ME, Wiertz E.** 2013. EBV BILF1 evolved to downregulate cell surface display of a wide range of HLA class I molecules through their cytoplasmic tail. J Immunol **190:**1672-1684.
14. **Croft NP, Shannon-Lowe C, Bell AI, Horst D, Kremmer E, Ressing ME, Wiertz EJ, Middeldorp JM, Rowe M, Rickinson AB, Hislop AD.** 2009. Stage-specific inhibition of MHC class I presentation by the Epstein-Barr virus BNLF2a protein during virus lytic cycle. PLoS Pathog **5:**26.

15. **Horst D, van Leeuwen D, Croft NP, Garstka MA, Hislop AD, Kremmer E, Rickinson AB, Wiertz EJ, Ressing ME.** 2009. Specific targeting of the EBV lytic phase protein BNLF2a to the transporter associated with antigen processing results in impairment of HLA class I-restricted antigen presentation. J Immunol **182:**2313-2324.
16. **Quinn LL, Zuo J, Abbott RJ, Shannon-Lowe C, Tierney RJ, Hislop AD, Rowe M.** 2014. Cooperation between Epstein-Barr virus immune evasion proteins spreads protection from CD8+ T cell recognition across all three phases of the lytic cycle. PLoS Pathog **10**.
17. **Pudney VA, Leese AM, Rickinson AB, Hislop AD.** 2005. CD8+ immunodominance among Epstein-Barr virus lytic cycle antigens directly reflects the efficiency of antigen presentation in lytically infected cells. J Exp Med **201:**349-360.
18. **Borza CM, Hutt-Fletcher LM.** 1998. Epstein-Barr virus recombinant lacking expression of glycoprotein gp150 infects B cells normally but is enhanced for infection of epithelial cells. J Virol **72:**7577-7582.
19. **Kurilla MG, Heineman T, Davenport LC, Kieff E, Hutt-Fletcher LM.** 1995. A novel Epstein-Barr virus glycoprotein gp150 expressed from the BDLF3 open reading frame. Virology **209:**108-121.
20. **Nolan LA, Morgan AJ.** 1995. The Epstein-Barr virus open reading frame BDLF3 codes for a 100-150 kDa glycoprotein. J Gen Virol **76:**1381-1392.
21. **Leung CS, Haigh TA, Mackay LK, Rickinson AB, Taylor GS.** 2010. Nuclear location of an endogenously expressed antigen, EBNA1, restricts access to macroautophagy and the range of CD4 epitope display. Proc Natl Acad Sci U S A **107:**2165-2170.
22. **Johnson JP, Demmer-Dieckmann M, Meo T, Hadam MR, Riethmuller G.** 1981. Surface antigens of human melanoma cells defined by monoclonal antibodies. I. Biochemical characterization of two antigens found on cell lines and fresh tumors of diverse tissue origin. Eur J Immunol **11:**825-831.
23. **Ben-Bassat H, Goldblum N, Mitrani S, Goldblum T, Yoffey JM, Cohen MM, Bentwich Z, Ramot B, Klein E, Klein G.** 1977. Establishment in continuous culture of a new type of lymphocyte from a "Burkitt like" malignant lymphoma (line D.G.-75). Int J Cancer **19:**27-33.
24. **Sabbah S, Jagne YJ, Zuo J, de Silva T, Ahasan MM, Brander C, Rowland-Jones S, Flanagan KL, Hislop AD.** 2012. T-cell immunity to Kaposi sarcoma-associated herpesvirus: recognition of primary effusion lymphoma by LANA-specific CD4+ T cells. Blood **119:**2083-2092.
25. **Rabin H, Hopkins RF, 3rd, Ruscetti FW, Neubauer RH, Brown RL, Kawakami TG.** 1981. Spontaneous release of a factor with properties of T cell growth factor from a continuous line of primate tumor T cells. J Immunol **127:**1852-1856.
26. **Barnstable CJ, Bodmer WF, Brown G, Galfre G, Milstein C, Williams AF, Ziegler A.** 1978. Production of monoclonal antibodies to group A erythrocytes, HLA and other human cell surface antigens-new tools for genetic analysis. Cell **14:**9-20.
27. **Young LS, Lau R, Rowe M, Niedobitek G, Packham G, Shanahan F, Rowe DT, Greenspan D, Greenspan JS, Rickinson AB, et al.** 1991. Differentiation-associated expression of the Epstein-Barr virus BZLF1 transactivator protein in oral hairy leukoplakia. J Virol **65:**2868-2874.
28. **Li D, Qian L, Chen C, Shi M, Yu M, Hu M, Song L, Shen B, Guo N.** 2009. Down-Regulation of MHC Class II Expression through Inhibition of CIITA Transcription by Lytic Transactivator Zta during Epstein-Barr Virus Reactivation. The Journal of Immunology **182:**1799-1809.
29. **Zuo J, Hislop AD, Leung CS, Sabbah S, Rowe M.** 2013. Kaposi's sarcoma-associated herpesvirus-encoded viral IRF3 modulates major histocompatibility complex class II (MHC-II) antigen presentation through MHC-II transactivator-dependent and -independent mechanisms: implications for oncogenesis. J Virol **87:**5340-5350.

30. **Tomazin R, Boname J, Hegde NR, Lewinsohn DM, Altschuler Y, Jones TR, Cresswell P, Nelson JA, Riddell SR, Johnson DC.** 1999. Cytomegalovirus US2 destroys two components of the MHC class II pathway, preventing recognition by CD4+ T cells. Nat Med **5:**1039-1043.
31. **Johannsen E, Luftig M, Chase MR, Weicksel S, Cahir-McFarland E, Illanes D, Sarracino D, Kieff E.** 2004. Proteins of purified Epstein-Barr virus. Proceedings of the National Academy of Sciences of the United States of America **101:**16286-16291.
32. **Coscoy L, Ganem D.** 2000. Kaposi's sarcoma-associated herpesvirus encodes two proteins that block cell surface display of MHC class I chains by enhancing their endocytosis. Proc Natl Acad Sci U S A **97:**8051-8056.
33. **Ishido S, Wang C, Lee BS, Cohen GB, Jung JU.** 2000. Downregulation of major histocompatibility complex class I molecules by Kaposi's sarcoma-associated herpesvirus K3 and K5 proteins. J Virol **74:**5300-5309.
34. **Ishido S, Goto E, Matsuki Y, Ohmura-Hoshino M.** 2009. E3 ubiquitin ligases for MHC molecules. Curr Opin Immunol **21:**78-83.
35. **Haque M, Ueda K, Nakano K, Hirata Y, Parravicini C, Corbellino M, Yamanishi K.** 2001. Major histocompatibility complex class I molecules are down-regulated at the cell surface by the K5 protein encoded by Kaposi's sarcoma-associated herpesvirus/human herpesvirus-8. J Gen Virol **82:**1175-1180.
36. **Lehner PJ, Hoer S, Dodd R, Duncan LM.** 2005. Downregulation of cell surface receptors by the K3 family of viral and cellular ubiquitin E3 ligases. Immunol Rev **207:**112-125.
37. **Brulois K, Toth Z, Wong LY, Feng P, Gao SJ, Ensser A, Jung JU.** 2014. Kaposi's sarcoma-associated herpesvirus K3 and K5 ubiquitin E3 ligases have stage-specific immune evasion roles during lytic replication. J Virol **88:**9335-9349.
38. **Bartee E, McCormack A, Fruh K.** 2006. Quantitative membrane proteomics reveals new cellular targets of viral immune modulators. PLoS Pathog **2**.
39. **Timms RT, Duncan LM, Tchasovnikarova IA, Antrobus R, Smith DL, Dougan G, Weekes MP, Lehner PJ.** 2013. Haploid genetic screens identify an essential role for PLP2 in the downregulation of novel plasma membrane targets by viral E3 ubiquitin ligases. PLoS Pathog **9:**21.
40. **Sanchez DJ, Gumperz JE, Ganem D.** 2005. Regulation of CD1d expression and function by a herpesvirus infection. J Clin Invest **115:**1369-1378.
41. **Thomas M, Boname JM, Field S, Nejentsev S, Salio M, Cerundolo V, Wills M, Lehner PJ.** 2008. Down-regulation of NKG2D and NKp80 ligands by Kaposi's sarcoma-associated herpesvirus K5 protects against NK cell cytotoxicity. Proc Natl Acad Sci U S A **105:**1656-1661.
42. **Li Q, Means R, Lang S, Jung JU.** 2007. Downregulation of gamma interferon receptor 1 by Kaposi's sarcoma-associated herpesvirus K3 and K5. J Virol **81:**2117-2127.
43. **Bartee E, Mansouri M, Hovey Nerenberg BT, Gouveia K, Fruh K.** 2004. Downregulation of major histocompatibility complex class I by human ubiquitin ligases related to viral immune evasion proteins. J Virol **78:**1109-1120.
44. **Ohmura-Hoshino M, Goto E, Matsuki Y, Aoki M, Mito M, Uematsu M, Hotta H, Ishido S.** 2006. A novel family of membrane-bound E3 ubiquitin ligases. J Biochem **140:**147-154.
45. **Ohmura-Hoshino M, Matsuki Y, Aoki M, Goto E, Mito M, Uematsu M, Kakiuchi T, Hotta H, Ishido S.** 2006. Inhibition of MHC class II expression and immune responses by c-MIR. J Immunol **177:**341-354.
46. **Hoer S, Smith L, Lehner PJ.** 2007. MARCH-IX mediates ubiquitination and downregulation of ICAM-1. FEBS Lett **581:**45-51.

678 47. **Nathan JA, Lehner PJ.** 2009. The trafficking and regulation of membrane receptors by the RING-
679 CH ubiquitin E3 ligases. Exp Cell Res **315:**1593-1600.
680 48. **Fogg MH, Carville A, Cameron J, Quink C, Wang F.** 2005. Reduced prevalence of Epstein-Barr
681 virus-related lymphocryptovirus infection in sera from a new world primate. J Virol **79:**10069-
682 10072.
683 49. **Wang F.** 2013. Nonhuman primate models for Epstein-Barr virus infection. Curr Opin Virol
684 **3:**233-237.
685
686

Funding Information:

This work was supported by grants from the Medical Research Council, London, UK (G0901755). The funders had no role in study design, data collection and interpretation, or the decision to submit the work for publication.

Acknowledgments: We thank for Dr Andrew Hislop for helpful discussions during this study.

Figure legends

Figure 1. Screening of EBV lytic genes to identify potential MHC class I immune evasion genes. MJS cells were transiently transfected with pCDNA3.1-IRES-GFP plasmids encoding for a selection of EBV lytic genes. At 24h post transfection surface levels of MHC class I (A) and MHC class II (B) on GFP positive cells were analysed using two color flow cytometry. (C) AKBM cells were induced into lytic cycle by cross-linking of B cell receptors for 1hr at 37ºC and analyzed at time points post-induction, as indicated, using western blot. Levels of BZLF1 protein (upper blot), BDLF3 protein (middle blot; stars indicate monomeric and trimeric BDLF3 protein) and, as a loading control, calregulin (lower blot) are shown.

Figure 2. BDLF3 expression induces the down regulation of surface MHC class I and MHC class II. MJS cells (A-D) and DG75 cells (E-H) were transiently transfected with control-GFP or BDLF3-GFP plasmids. At 24h post transfection, two color flow cytometry was used to measure surface levels of MHC class I (A,E), MHC class II (B,F), TfR (C,G) and ICAM1 (D) or CD19 (H) in the GFP^+ populations of control-GFP (solid line histogram), and BDLF3-GFP transfected cells (dashed line histogram). The grey histogram denotes background staining obtained with an isotype control antibody.

Figure 3. BDLF3 induces downregulation of all HLA class I and class II alleles. (A) The MHC class I negative cell line K562 transduced to stably express either HLA-A2, -B35 or -Cw1 was electroporated with control-GFP or BDLF3-GFP plasmids. At 24h post-transfection, two color flow cytometry was used to measure surface MHC class I levels in the GFP^+ populations in the control-GFP transfected (solid line histogram) and

717 the BDLF3-GFP transfected cells (dashed line). (B) HEK-293 cells stably expressing
718 CIITA were transiently transfected with control-GFP or BDLF3-GFP plasmids. At 24h
719 post-transfection, two color flow cytometry was used to measure surface HLA-DR and
720 HLA-DQ levels in GFP^+ populations in the control-GFP transfected (solid line histogram)
721 and the BDLF3-GFP transfected cells (dashed line). The grey histogram denotes
722 background staining obtained with an isotype control antibody.

723 **Figure 4. BDLF3 can inhibit EBV specific $CD8^+$ and $CD4^+$ T cell recognition.** MJS
724 cells were co-transfected with p509 plasmid (BZLF1 expression vector) together with
725 control-GFP or BDLF3-GFP. At 24h post transfection, the MJS cells were co-cultured
726 with effector T cells, BZLF1 (RAK)-specific $CD8^+$ T cell clone, for a further 18hr and the
727 supernatants were tested for the release of IFN-γ as a measure of T cell recognition. All
728 results are expressed as IFN-γ release in pg/ml and error bars indicate standard
729 deviation of triplicate cultures. (B) Total cell lysates were generated from the above
730 transfections, and analyzed by western blotting using antibodies specific for BDLF3,
731 BZLF1 or calregulin as a loading control. The asterisks adjacent to the BDLF3 blot
732 indicate monomeric and trimeric BDLF3 protein. (C) MJS-DR51 cells were first
733 transfected with EBNA1ΔNLS, allowed to recover in culture overnight, then were divided
734 to two groups and transfected with either BDLF3-NGFR or Control-NGFR. After a
735 further 24h, $NGFR^+$/$BDLF3^+$ or control $NGFR^+$ cells were sorted with magnetic beads
736 and used as targets for HLA-DR51 restricted EBNA1 (SNP) specific $CD4^+$ T cell clones.
737 Recognition was measured as pg/ml of IFN-γ release by T cell clones. Error bars
738 represent standard deviation of the mean for triplicate assay replicates. Results are

representative of three independent experiments. (D) Total cell lysates were generated from the above transfections, and analyzed by western blotting using antibodies specific for BDLF3, EBNA1 or calregulin as a loading control.

Figure 5. BDLF3 induces a more dramatic reduction in surface MHC class I and II compared to whole cell levels. (A) MJS cells were transiently transfected with control-GFP or BDLF3-GFP plasmids. At 24h post transfection, two color flow cytometry was used to measure the level of surface MHC class I (upper left), MHC class II (middle left) and ICAM1 (lower left) in the viable GFP^+ populations of control-GFP transfected (solid line histogram), and BDLF3-GFP transfected cells (dashed line histogram). The grey histogram denotes background staining obtained with an isotype control antibody. In parallel, these GFP^+ transfected MJS cells were analysed for whole cell levels of MHC class I (upper right), MHC class II (middle right) and ICAM1 (lower right) using intracellular staining of fixed and permealized cells. The results are representative of repeated experiments. (B) Relative mean fluorescence intensity (MFI) of MHC class I, MHC class II and ICAM1 in BDLF3-GFP^+ cells compared to control-GFP^+ cells were calculated. Results are the combined data from three independent experiments. White bars represent surface staining, grey bars represent whole cell staining. Differences that reached significance ($p<0.05$) in a Student's Paired T test are denoted by an asterisk.

Figure 6. BDLF3 induces more rapid internalization and delayed appearance of both MHC class I and class II at the cell surface. Internalization and appearance assays were performed on MJS cells transiently expressing control-GFP or BDLF3-GFP. The GFP^+ population was used to gate on BDLF3 expressing cells. Internalization

761 and appearance assays were performed on cells pre-treated on ice with saturating
762 amounts of anti-MHC class I antibody or anti-MHC class II antibody. Cells were then
763 washed and incubated at 37°C for up to 60 min. (A) For the internalization assay, viable
764 cells harvested at each time point were stained with APC-conjugated goat anti-mouse
765 IgG antibody, and analyzed using flow cytometry at the indicated times; this identifies
766 the pre-labeled antibody-bound MHC molecules that remain at the surface while
767 endocytosed labeled MHC molecules are not detected on the viable cells. The mean
768 fluorescence intensities of staining were averaged for triplicate samples, and then
769 normalized to the time 0 samples. (B) For the appearance assays, newly-arrived MHC-I
770 and MHC-II molecules, which were not prelabeled with unconjugated antibodies, were
771 detected by staining with APC-conjugated anti-MHC class I antibody or anti-MHC class
772 II antibody. The mean fluorescence intensities of staining were averaged for triplicate
773 samples, and then normalized to the time 0 samples. Results are representative of
774 three independent experiments.

775 **Figure 7. Treatment of BDLF3 expressing cells with a proteasome inhibitor**
776 **prevents down regulation of MHC class I and class II**. MJS cells were transiently
777 transfected with BDLF3-GFP or control-GFP plasmids, and then incubated in normal
778 medium (A) or with MG132 (5μM) supplemented medium (B). At 24h post-transfection,
779 two color flow cytometry was used to measure surface MHC class I (upper histograms),
780 surface MHC class II (middle histograms) and surface ICAM1 (lower histograms) in
781 GFP^+ populations of control-GFP (solid line histogram), and BDLF3-GFP (dashed line
782 histogram) transfected cells. The grey histogram denotes background staining obtained

783 with an isotype control antibody. Results are representative of repeated experiments
784 (n>4). (C,D) MJS cells were transiently transfected with BDLF3-GFP or control-GFP
785 plasmids, and then were incubated with MG132 (5μM). Following drug treatment, the
786 rate of internalization (C) of MHC-I (top panel) and MHC-II (bottom panel), and the rate
787 of appearance (D) of MHC-I (top panel) and MHC-II (bottom panel) were measured
788 using the same method as in Fig. 6. (E, F) MJS cells were transfected with a ubiquitin
789 expression plasmid plus either Control-NGFR or BDLF3-NGFR plasmids; these
790 transfected cells were then divided in to two and incubated in normal medium or in
791 medium supplemented with MG132. At 24h post transfection, $NGFR^+$/$BDLF3^+$ or control
792 $NGFR^+$ cells were sorted with magnetic beads, and surface MHC class I (C) or MHC
793 class II (D) were immunoprecipitated, eluted, and then immunoblotted using anti-
794 ubiquitin antibody (P4D1).

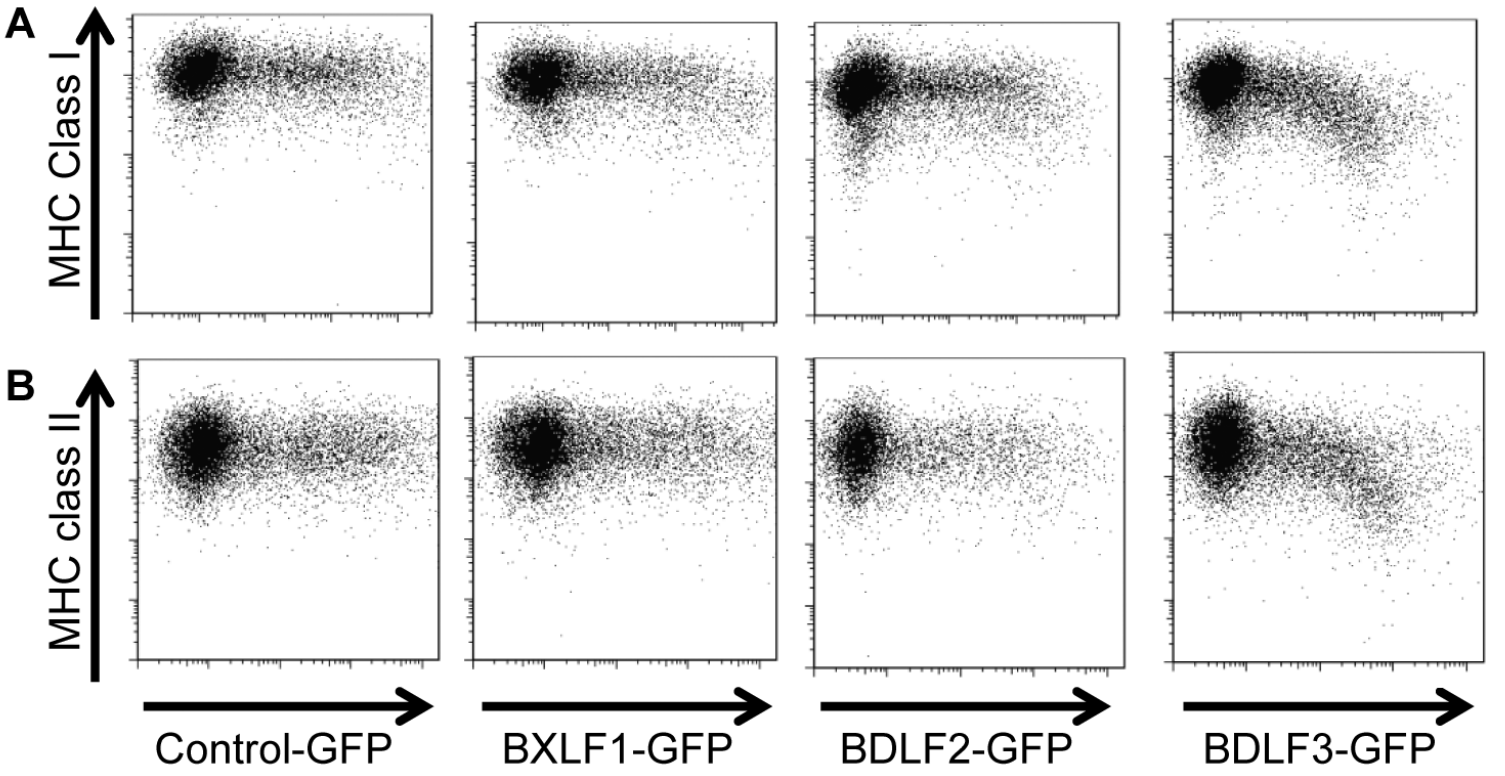
A
MHC Class I
B
MHC class II
Control-GFP
BXLF1-GFP
BDLF2-GFP
BDLF3-GFP

C

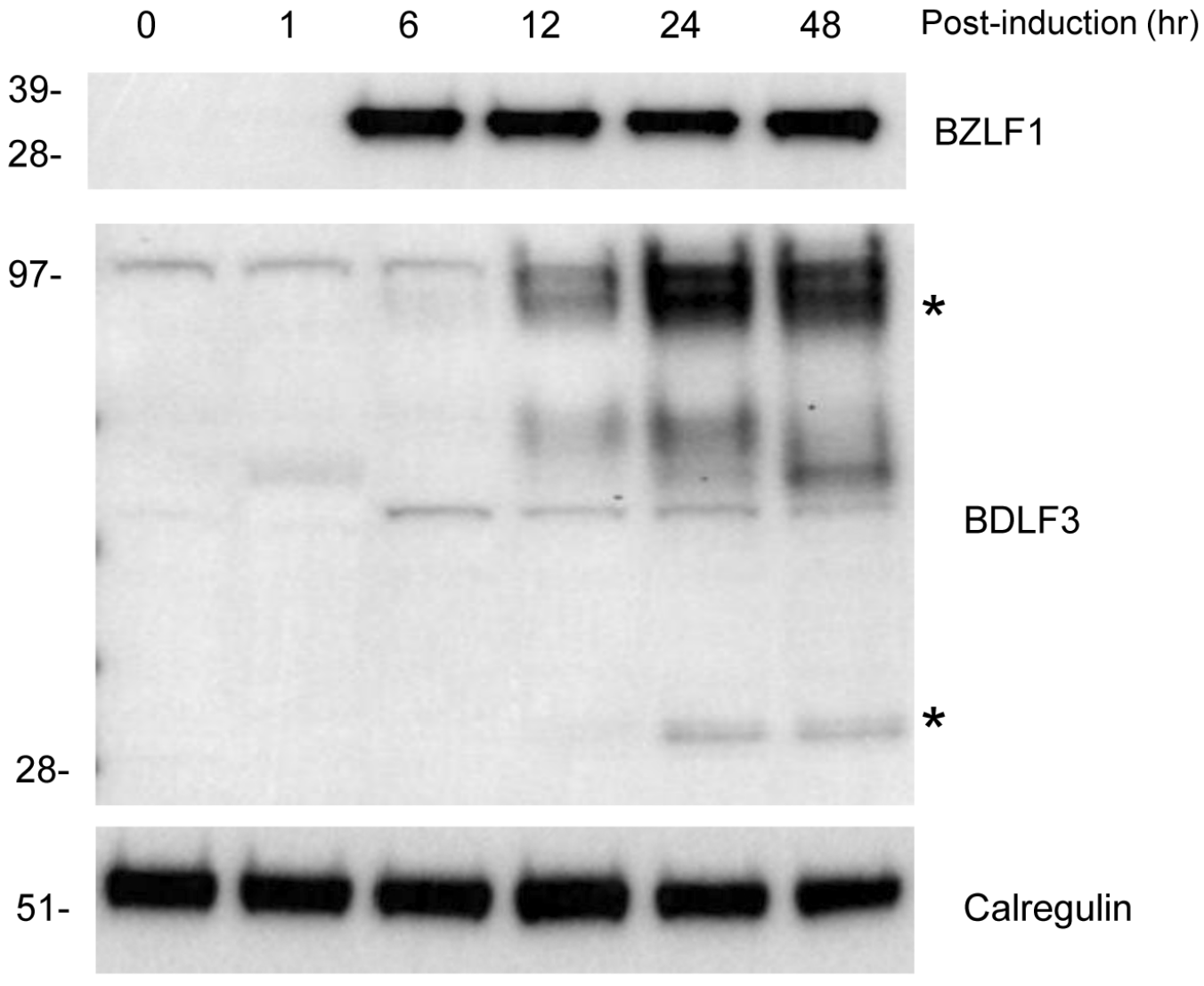
0
1
6
12
24
48
Post-induction (hr)
39-
28-
BZLF1
97-
*
BDLF3
*
28-
51-
Calregulin

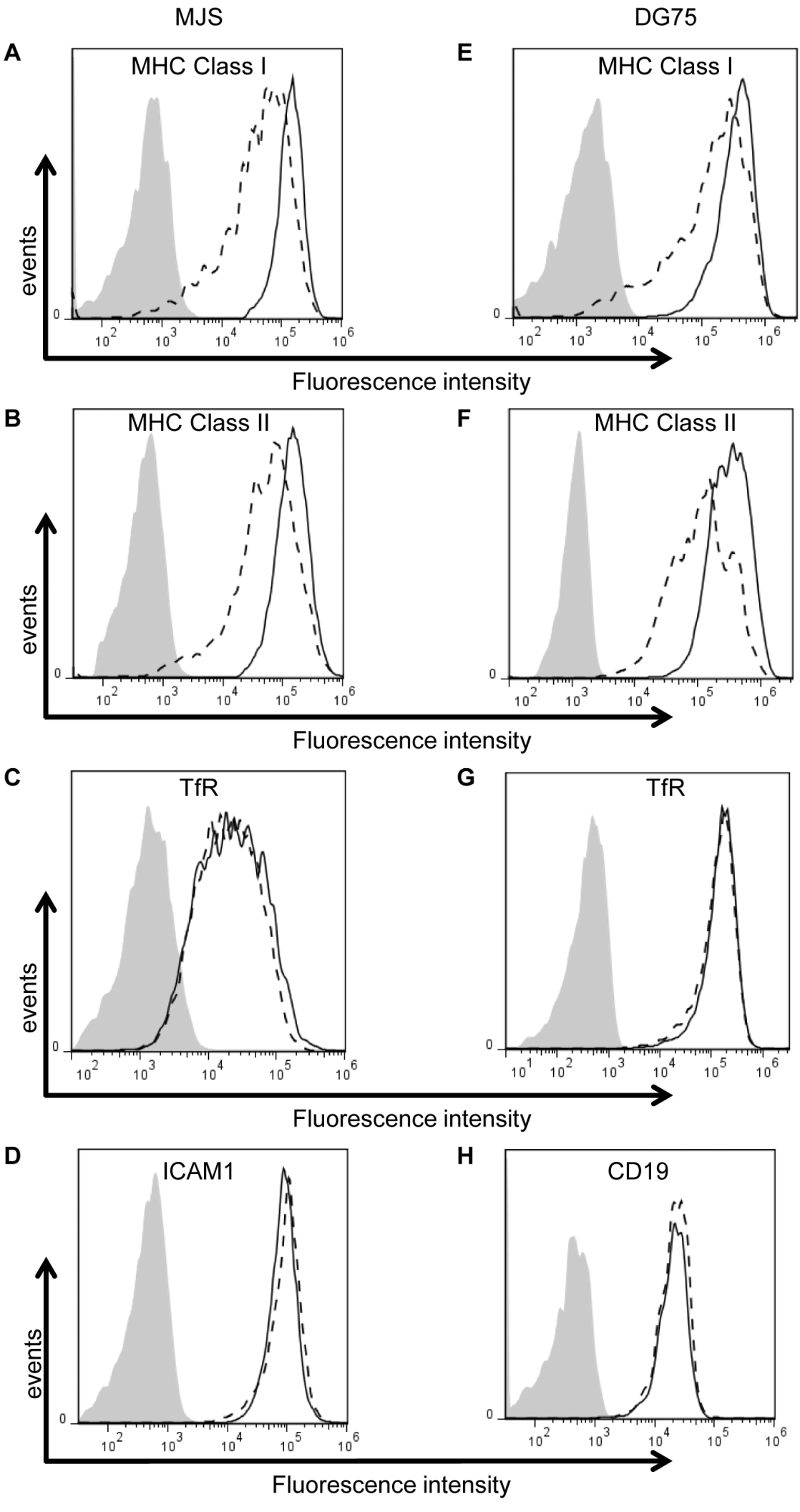
MJS
DG75
A
MHC Class I
E
MHC Class I
events
Fluorescence intensity
B
MHC Class II
F
MHC Class II
events
Fluorescence intensity
C
TfR
G
TfR
events
Fluorescence intensity
D
ICAM1
H
CD19
events
Fluorescence intensity

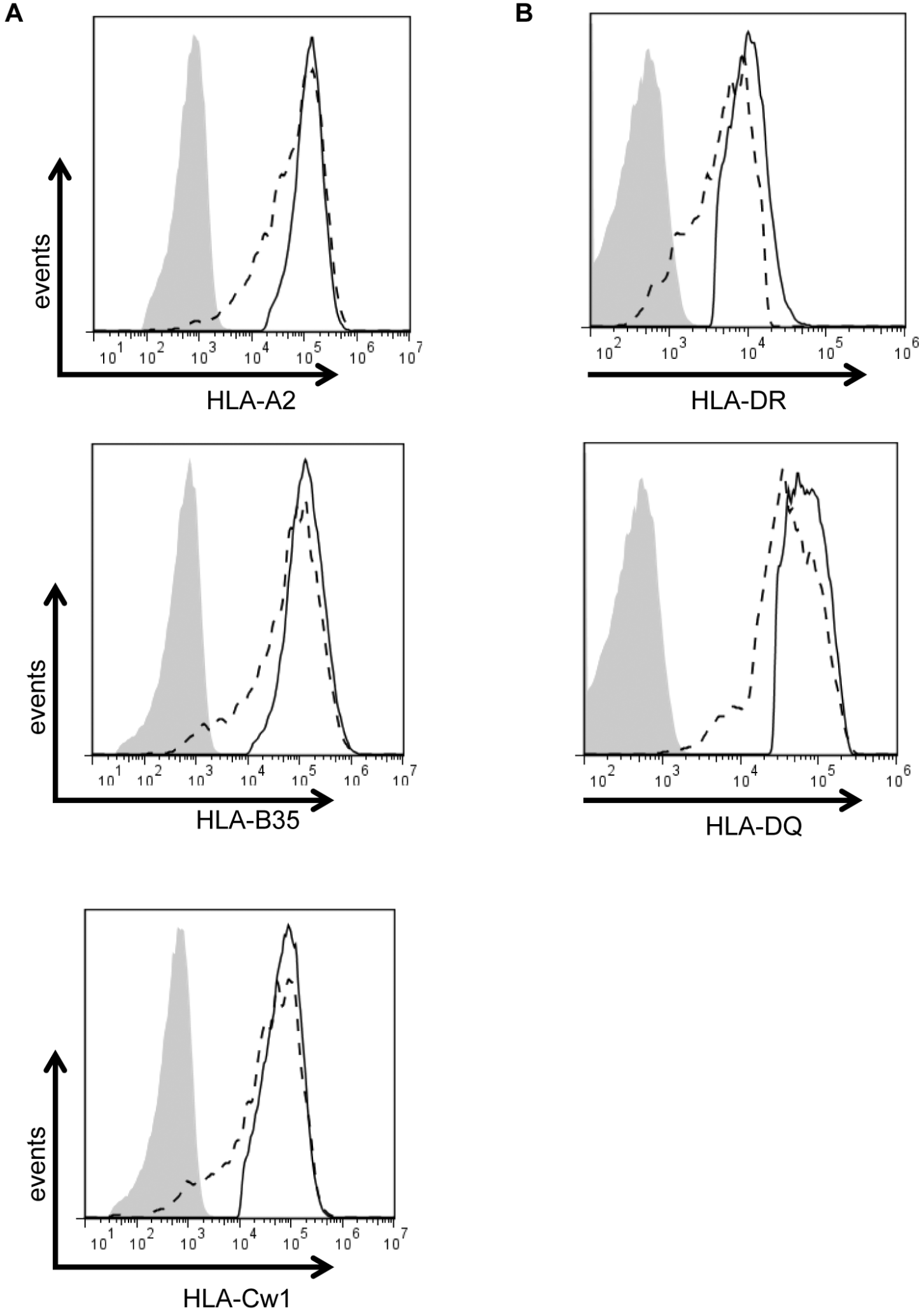
A
events
HLA-A2
B
HLA-DR
events
HLA-B35
HLA-DQ
events
HLA-Cw1

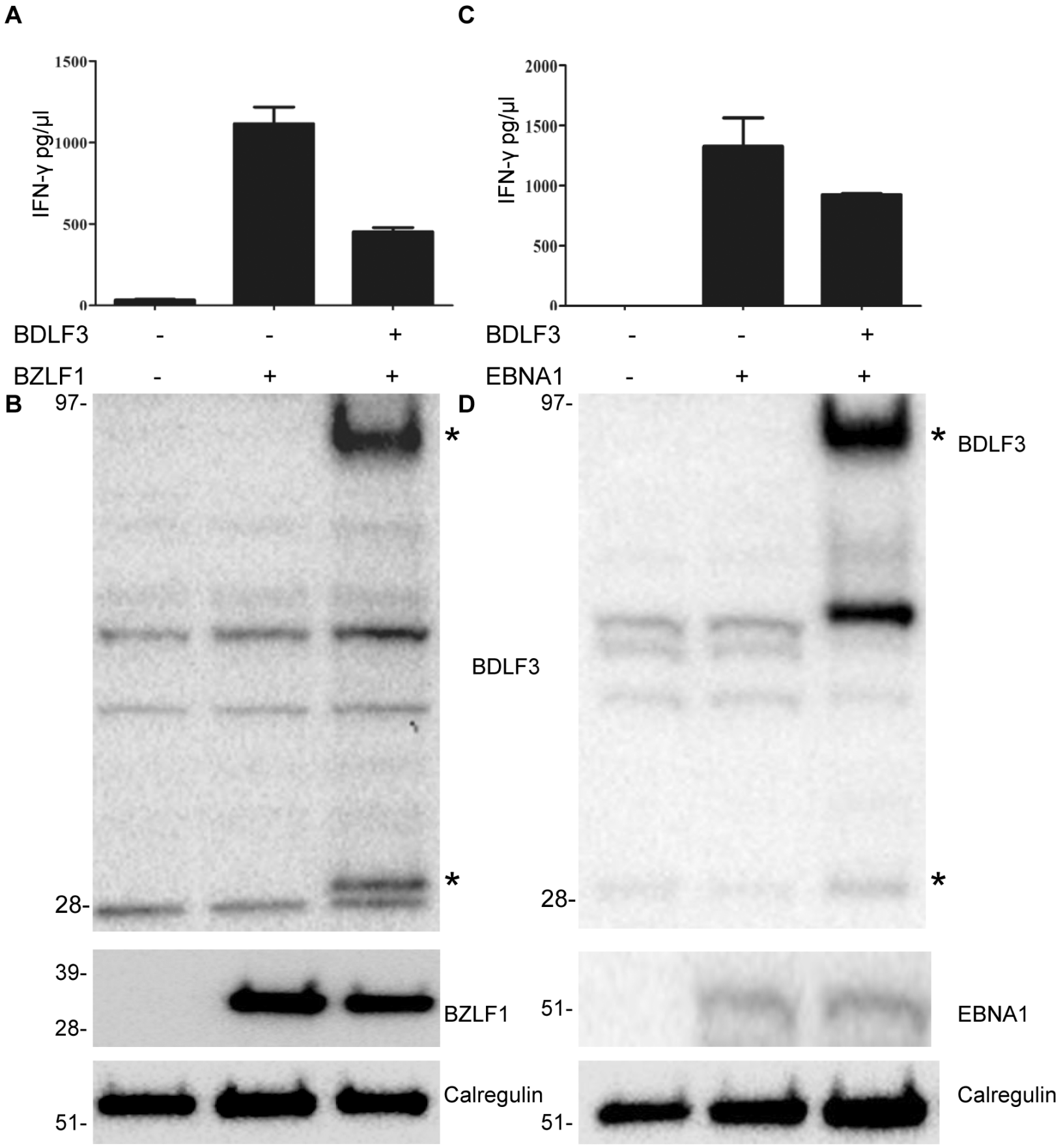
A
IFN-γ pg/μl
1500
1000
500
0
BDLF3 - - +
BZLF1 - + +
C
IFN-γ pg/μl
2000
1500
1000
500
0
BDLF3 - - +
EBNA1 - + +
B
97-
28-
*
*
39-
28-
BZLF1
51-
Calregulin
D
97-
28-
*
*
BDLF3
BDLF3
51-
EBNA1
51-
Calregulin

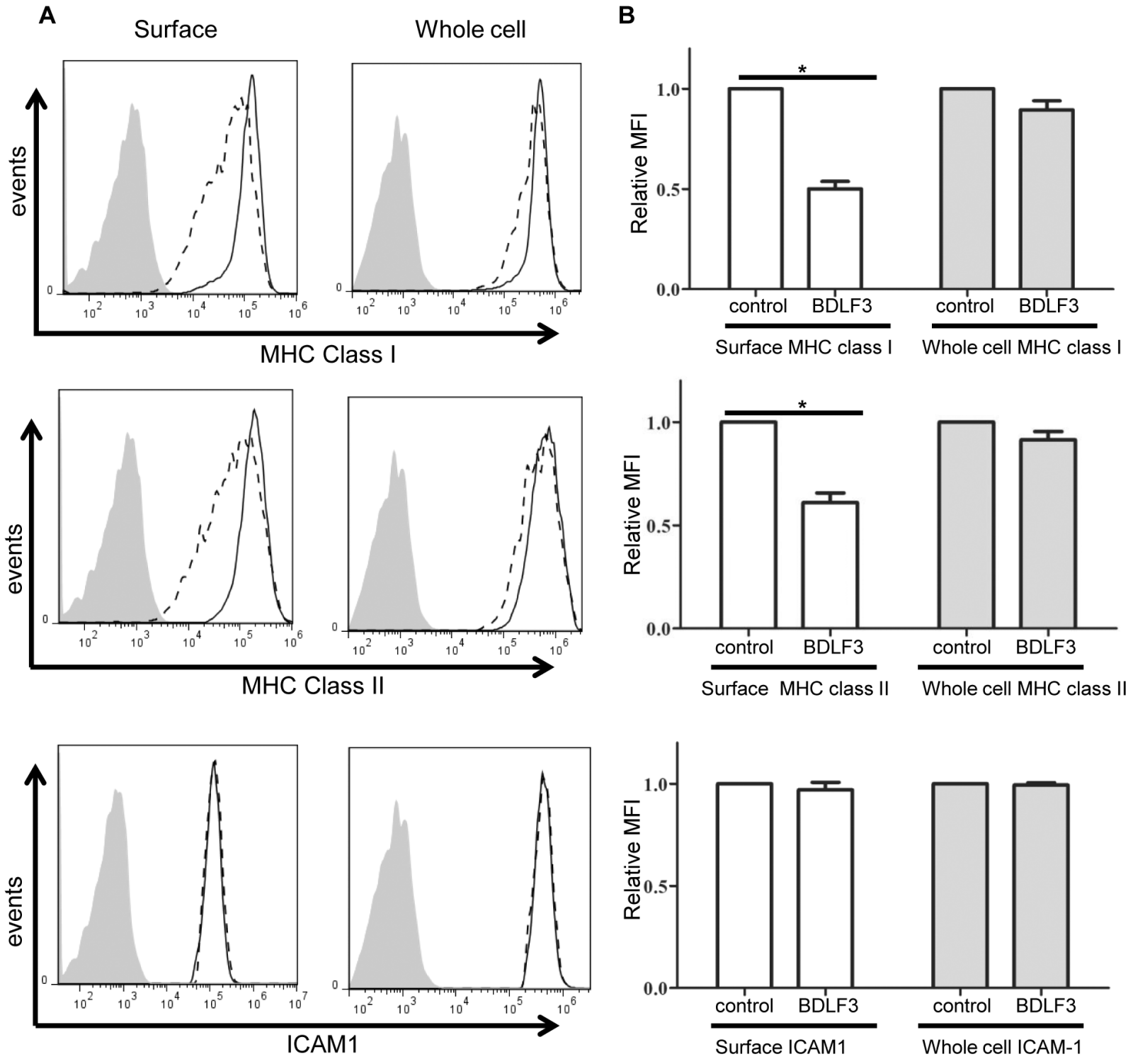
A
Surface
Whole cell
events
MHC Class I
MHC Class II
ICAM1
B
Relative MFI
control
BDLF3
Surface MHC class I
Whole cell MHC class I
Surface MHC class II
Whole cell MHC class II
Surface ICAM1
Whole cell ICAM-1

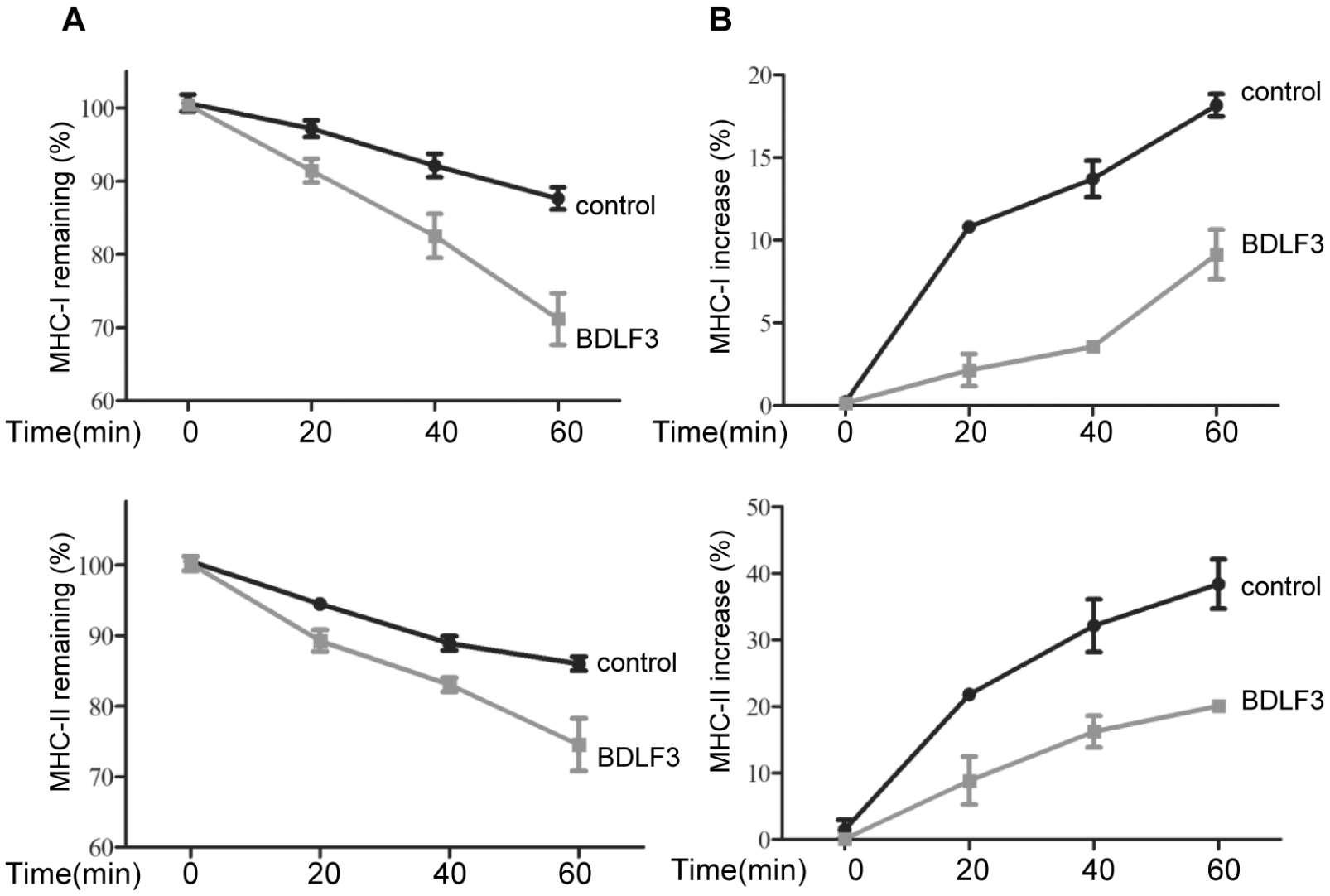
A
B
MHC-I remaining (%)
100
90
80
70
60
control
BDLF3
Time(min)
0
20
40
60
MHC-I increase (%)
20
15
10
5
0
control
BDLF3
Time(min)
0
20
40
60
MHC-II remaining (%)
100
90
80
70
60
control
BDLF3
Time(min)
0
20
40
60
MHC-II increase (%)
50
40
30
20
10
0
control
BDLF3
Time(min)
0
20
40
60

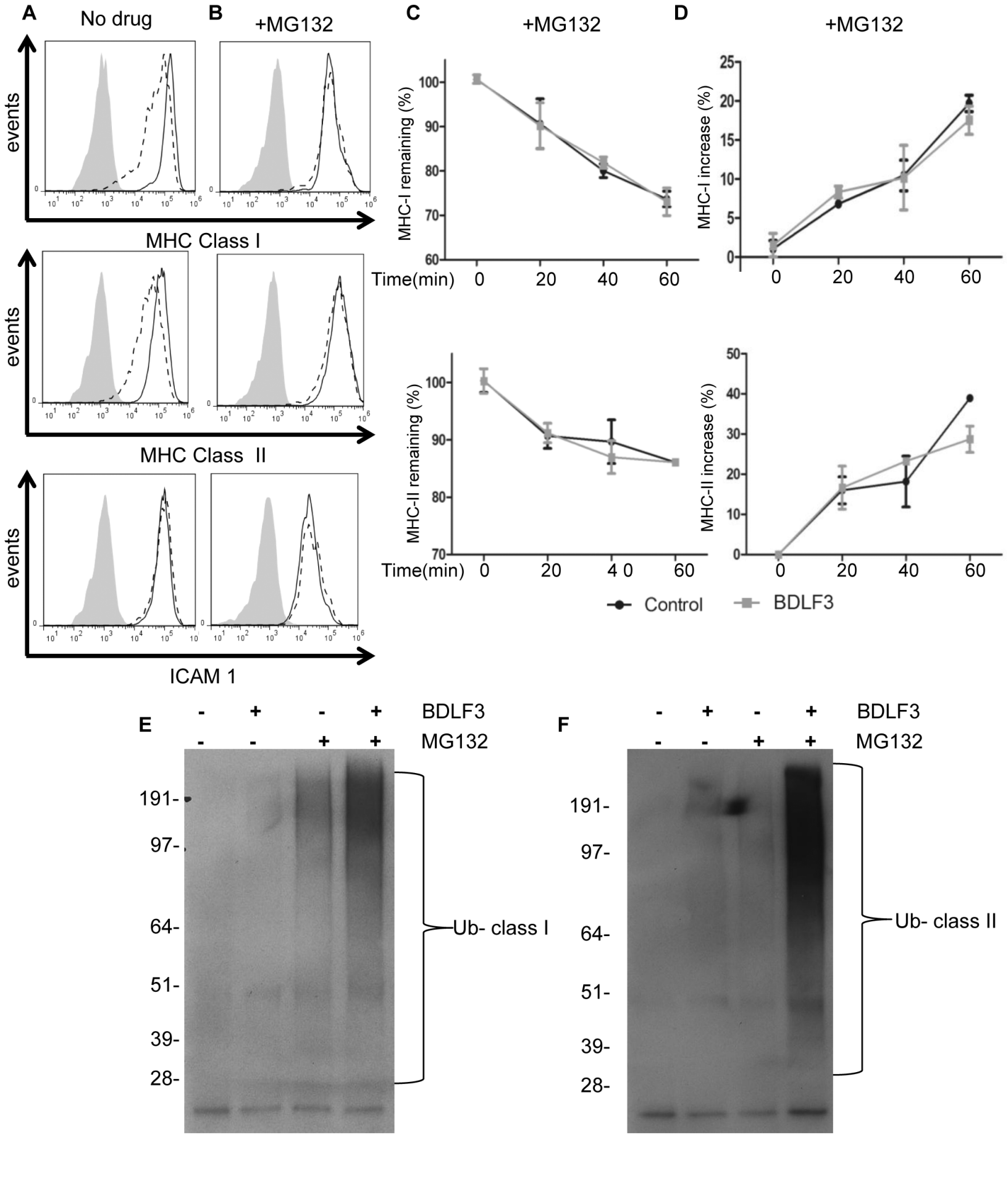
A
No drug
B
+MG132
C
+MG132
D
+MG132
events
MHC Class I
MHC Class II
ICAM 1
MHC-I remaining (%)
MHC-I increase (%)
MHC-II remaining (%)
MHC-II increase (%)
Time(min)
Control
BDLF3
E
F
BDLF3
MG132
191-
97-
64-
51-
39-
28-
Ub- class I
Ub- class II